Cureus Journal of Engineering

Open Access Original Article

KneExo: Design, Development, and Functional Evaluation of a Bio-joint Shaped Knee Exoskeleton for Sit-to-Stand Assistance

Received 09/23/2024
Review began 09/30/2024
Review ended 01/23/2025
Published 01/28/2025

DOI:
https://doi.org/10.7759/s44388-024-00636-x

Omid Arfaie [1] , Ramazan Unal [1]

1. Department of Mechanical Engineering, Human-Centered Design Laboratory, Ozyegin University, Istanbul, TUR

Corresponding authors: Omid Arfaie, omid.arfaie@ozu.edu.tr, Ramazan Unal, ramazan.unal@ozyegin.edu.tr

Abstract

In addressing age-related muscle strength decline among elderly individuals, the development of assistive devices for daily living becomes imperative. This paper introduces a passive knee exoskeleton designed to aid older adults during sit-to-stand (STS) tasks. Inspired by the knee joint biomechanics encompassing rotational and translational motions, this exoskeleton employs a cam mechanism. This mechanism facilitates thigh rotation within a linear slot, adjusting the exoskeleton's rotational center and effectively minimizing misalignment with the user's knee joint. As the upper part attached to the thigh rotates within the cam mechanism, a spring in the lower part attached to the shank is compressed via a crank, storing energy during the sitting phase and releasing it during standing.

The evaluation of this exoskeleton involves using an instrumented chair to collect force data from the hands during the STS tasks. Additionally, the muscle activities of the lower limb are measured during the evaluations. According to the initial functional evaluation, the developed knee exoskeleton (KneExo) provides 31.76% and 29.24% assistance w.r.t. body weight for the unloaded and loaded (20 kg load in the backpack), respectively.

The sEMG results indicate the most reduction in muscle activity for the tibialis anterior (TA) muscles. Specifically, there is a 19.2% decrease in muscle activity in the left TA and a 31.2% decrease in the right TA for the unloaded and loaded cases, respectively.

Implementing the human-inspired design in the proposed KneExo exhibits a substantial 51% reduction in misalignment with the user's knee joint compared to a revolute joint. This underscores its potential as an effective assistive device for elderly individuals coping with diminished muscle strength.

Categories: Biotechnology and Engineering, Design and Manufacturing
Keywords: assistive device, rehabilitation, biomechanics, knee exoskeleton, sit-to-stand

Introduction

It is estimated that, by 2030, one in six people globally, with a total of 1.4 billion, will be aged 60 or older. By 2050, this demographic is expected to double, reaching 2.1 billion individuals aged 60 and above [1]. Aging causes the loss of muscle fibers, decreasing muscle strength capacities and metabolism [2]. Consequently, reduced muscle power may increase the risk of falling by decreasing the postural stability in older adults [3,4]. In these individuals, the strength of the muscles reduces by 12-15% every decade [5]. Among the human activities of daily living (ADL), the sit-to-stand (STS) movement is one of the repetitive ones. For instance, standing up from a chair is an activity that is repeated daily for several times. Lower limb muscles such as the quadriceps, tibialis anterior, hamstrings, and glutes contribute to this ADL [6]. Aged people exhibit more muscle activities of the lower limb muscles during the STS task [7].
Several research studies are conducted to design assistive devices to help older people with ADL [8-10]. These devices, such as Indego Exoskeletons [8], can aid individuals with muscle weakness and influence the postural controls and upper body postures [8]. These assistive devices are classified as passive and active devices. Passive elements, such as mechanisms with elastic elements, are employed in passive devices for assistance. In active devices, external power is injected via actuators, i.e., D.C. motors. For instance, Beyl et al. introduced KNEXO, utilizing pleated pneumatic artificial muscles to offer adjustable knee joint support [11]. Kong et al. employed a rotary series elastic actuator (SEA) for precise torque generation during gait rehabilitation [12], while FUM-KneeExo and other models incorporated linear SEAs for knee joint assistance [13,14].

The selection of materials is crucial in lower limb exoskeleton design, with choices between soft materials, like textiles and thermoplastic composites, and hard materials, such as aluminum, steel, and titanium, each impacting comfort and durability. Soft exoskeletons, such as Xosoft [15] and SR-AFO [16], use flexible materials for variable stiffness and comfort, while rigid frames, like those in ReWalk [17] and Lokomat [18], rely on metals for strength and precision. Recent advances in materials, including the implementation of carbon fiber and 3D-printed composites in exoskeletons such as KAFO [19], offer promising weight reduction benefits, though challenges remain in achieving the desired shapes and long-term durability.

While active exoskeletons fulfill the varying requirements of different ADL, there is higher mass and complexity within these systems. Moreover, their reliance on batteries often limits the operational duration. Consequently, some researchers advocate for passive exoskeletons to address these constraints, aiming for lighter, more compact designs with reduced complexity. Libo Zhu et al. [9] propose a passive lower-limb exoskeleton to compensate for gravity, including springs, gears, and a lead screw nut mechanism to convert the axial forces into the torques on the hip and knee joints. Kong et al. present a tendon-driven exoskeleton to assist patients and older people in carrying heavy objects [10]. Diego Felipe et al. propose a passive exoskeleton to assist the STS transition with a torso lifting mechanism [20]. This exoskeleton can reduce more than 30% of the muscle activities involved in this transition.

Although passive exoskeletons assist elderly individuals with their ADL, addressing the misalignment between these exoskeletons and the body's joints remains a significant challenge in designing lower-body exoskeletons. The biomechanics of the knee joint encompass rotational and sliding motions [21], maintaining a specific ratio between these movements [22]. Damiano Zanotto et al. [23] investigate the human-robot interaction forces and how these forces affect gait kinematics and timing using experiments with healthy subjects walking in the ALEX II exoskeleton. The results show that the knee misalignment significantly influenced interaction forces, especially at the thigh interface. Previous studies emphasize the significance of a cam mechanism, which is crucial in providing both rotational and sliding motions to replicate human activities like walking or STS motions [24,25]. Dong Jin Hyun et al. [26] propose an active lower-limb exoskeleton that utilizes a powered artificial knee joint with a double four-bar structure that can generate polycentric knee motion. This powered knee structure yields the human-robot knee alignment during leg motion. Guotao Li et al. [27] propose a spatial self-aligning mechanism in the knee joint that assists both flexion/extension (F/E) in the knee and internal/external rotation in the hip joint. Additionally, the exoskeleton can adapt to the variations in the knee's instantaneous rotation center to compensate for the misalignment. Donghai Wang et al. [28] assessed five distinct knee exoskeleton designs to explore the significance of adaptive kinematic components and the effects of the knee rolling/sliding mechanism. The findings indicate that employing a pin slider/cam mechanism effectively replicates the geometry of the human knee joint and reduces internal joint forces resulting from human-exoskeleton interaction.

Although the mentioned studies address the solutions for solving the misalignment challenges by providing different designs and mechanisms, they all use active actuators to assist the user during different ADLs. Additionally, since muscle activity is crucial in older adults, the potential for these exoskeletons to reduce muscle activity as an indicator of metabolic effort has not been investigated. Addressing these limitations, this paper presents a passive mechanism tailored to aid older individuals and those with weakened muscles by providing support of up to 25% of their body weight, alleviating the strain on their muscles. To replicate the natural behavior of the knee joint during the STS task, we implement a cam mechanism based on the concept we proposed in our previous study [29] to minimize misalignment between the knee exoskeleton and the user's knee joint by integrating. An instrumented chair equipped with four load cells, meticulously designed to capture the distribution of forces during the STS cycle, is developed for the functional evaluation of the KneExo. Additionally, the muscle activities during the STS cycle with KneExo and without KneExo are measured and compared using the sEMG sensors.

Materials And Methods

Mechanical and conceptual design

Based on the findings in [30], since the peak torque in the knee joint is significantly higher in the sagittal plane than in the frontal and transverse planes, this study focuses on kinematic and kinetic analyses in the sagittal plane. According to the results of kinematic and kinetic analyses during the STS task of healthy subjects [31], the range of motion (RoM) of the knee joint and the required knee torque are approximately 79° and 0.7 N·m/kg, as depicted in Figure *1*. Analyzing the kinetics of sitting suggests an opportunity to utilize potential energy that can be stored and subsequently released during the standing phase. Thus, elastic elements can be implemented to store energy while sitting.

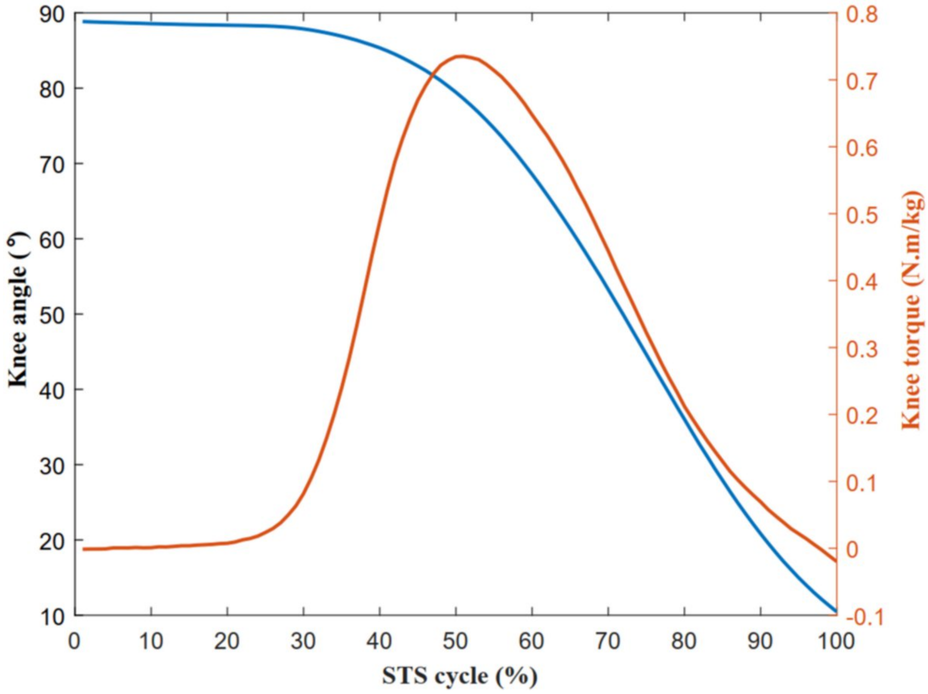

FIGURE 1: Kinematic and kinetic analyses during STS task of the healthy subjects

STS, sit-to-stand

In previous studies, several design solutions have been proposed to address the challenges of knee joint misalignment in exoskeletons, particularly due to the complex biomechanics involving both rotational and translational movements of the femur and tibia [32]. One prominent approach is using a bio-joint shaped cam mechanism, which mirrors the knee's non-uniform geometry. During flexion and extension, the femoral and tibial condyles rotate and slide relative to each other. This bio-inspired design allows the exoskeleton to follow the natural movement of the knee joint, minimizing internal forces and torques exerted on the knee and enhancing the interaction between the human joint and the exoskeleton for improved comfort and performance [29].

Building on these principles, the current design incorporates a linear slot in the lower link to prevent misalignment of the bio-joint's rotation center and account for the varying length of the shank relative to the femur. As the lateral compartment of the femur rotates and slides on the tibia, the cam slot path is designed to follow the sagittal profile of this motion. The length of the linear slot is determined by the displacement between the exoskeleton's rotation center and the cam rollers, reaching a maximum of 15 mm at full flexion and reducing to 10 mm at 90°, corresponding to the posterior translation of the femur on the tibia. The 2D sketch of the proposed concept is shown in Figure *2*.

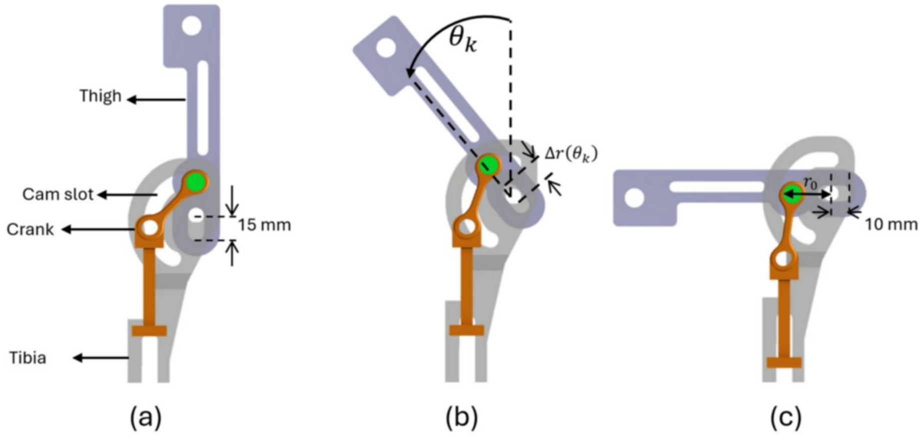

FIGURE 2: The working principle of the bio-joint shaped knee mechanism of the KneExo (green point indicates the moving of the cam design profile), full extension of the knee joint in the standing position (a), flexion of the knee joint during the STS task (b), full flexion of the knee joint in the sitting position (c)

STS, sit-to-stand

To model the kinematics of the cam design, the parametric equations governing the cam slot path are determined as follows:

$$x_{cam}(\theta_k) = (r_0 + \Delta r(\theta_k)) \cdot \cos(\theta_k)$$

$$y_{cam}(\theta_k) = (r_0 + \Delta r(\theta_k)) \cdot \sin(\theta_k)$$

As shown in Figure 2, in these equations, r_0 is the initial radius of curvature at 90° of flexion, and $\Delta r(\theta_k)$ represents the posterior translation, varying between 10 mm and 15 mm as the knee moves through flexion. The function $\Delta r(\theta_k)$ is modeled as follows:

$$\Delta r(\theta_k) = 10\text{mm} + \frac{5}{\theta_{max}} \cdot (\theta_k - 90^\circ)$$

where θ_{max} is the maximum flexion angle. This ensures that the cam roller moves along a path corresponding to the natural knee motion, accounting for both rotational and translational movements. The simulated cam slot profile is shown in Figure 3, where the initial radius of curvature and maximum flexion are considered 80 mm and 120°.

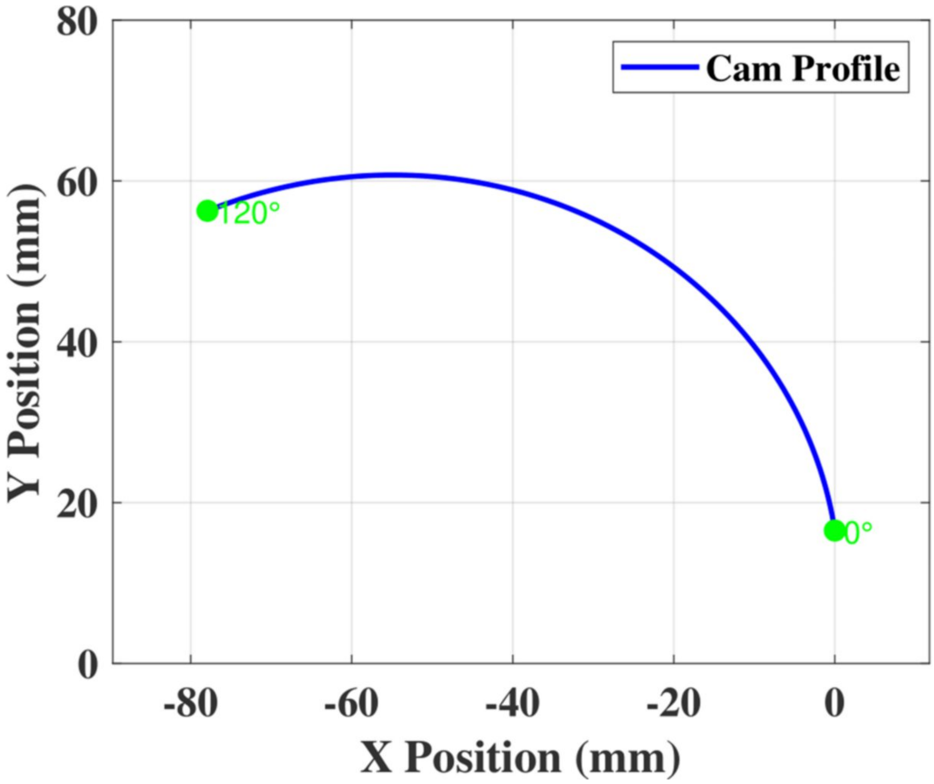

FIGURE 3: The simulated cam slot profile

The cam mechanism functions by translating horizontal and vertical displacements into deflections of a compression spring located in the lower link. This spring stores energy during the weight acceptance phase and releases it during extension. The displacement between the exoskeleton's rotation center and the cam rollers, extending to 15 mm during full flexion and reducing to 10 mm at 90° flexion, plays a crucial role in minimizing misalignment and improving the exoskeleton's mechanical efficiency. These values correspond to the posterior translation of the femur relative to the tibia, as elucidated in [33].

The proposed exoskeleton in this paper comprises three primary components: the thigh link, the bio-joint shaped mechanism, and the shank link. These parts are designed based on the conceptual framework, and their dimensions are obtained from anthropomorphic body segment lengths according to the Gait2392 model of OpenSim [34]. The CAD model of the proposed KneExo is depicted in Figure *4* and includes tibia and thigh links, as well as compression springs, connecting braces to the body, and a crank part that is responsible for transferring energy from the elastic element to the knee joint. The KneExo is connected to the body through three position-adjustable supporting braces.

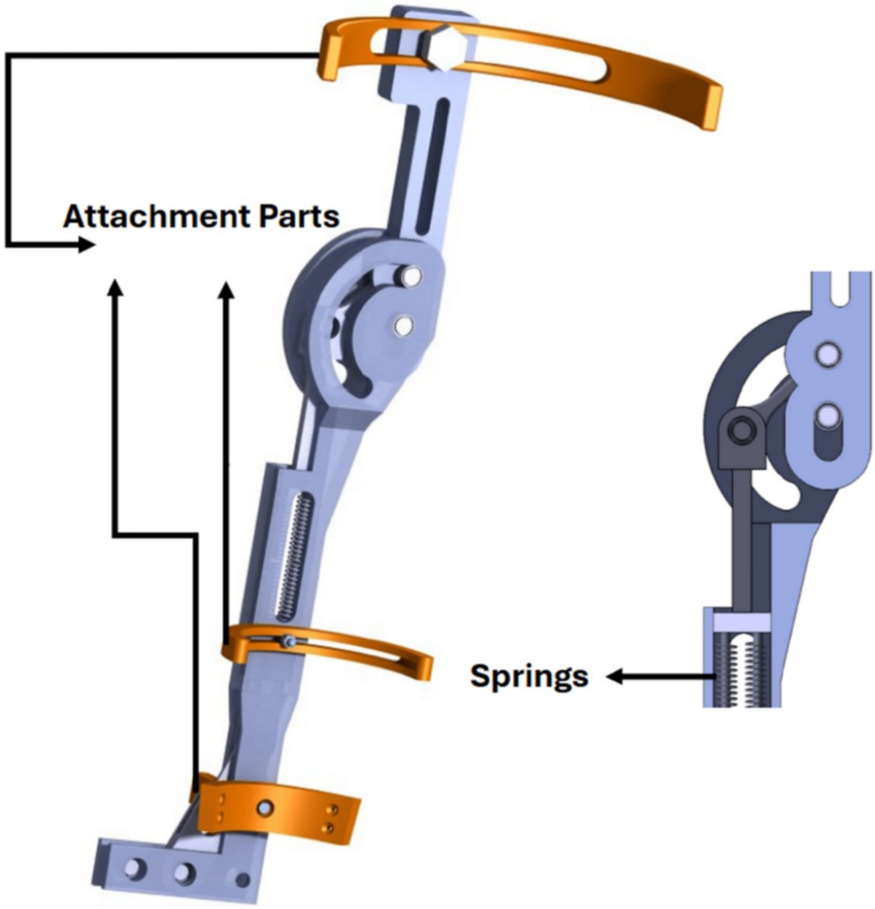

FIGURE 4: CAD model of the KneEXo (left), braces are implemented to fit the KneExo to the lower limb, and the springs are placed inside the shank part (right)

Kinematic and kinetic analyses

The kinematic and kinetic analyses in this study examine the movement of the knee joint and the forces exerted by the exoskeleton during the STS task. Referring to Figure 4, the arm r_m directly transmits the generated force within the elastic element encased within the shank, exerting torque around the knee joint. The magnitude of the moment arm vector dynamically alters with the knee joint's flexion/extension and is determined as follows:

$$r_m = r\cos\theta_k$$

Here, r denotes the radius of the cam slot, while θ_k represents the knee joint angle. The schematic diagram illustrating the corresponding cam slot mechanism and the KneExo during the knee joint flexion is depicted in Figure 5. Notably, the maximum value of the moment arm occurs when the subject is seated, whereas it diminishes to zero when the body is in a stance position.

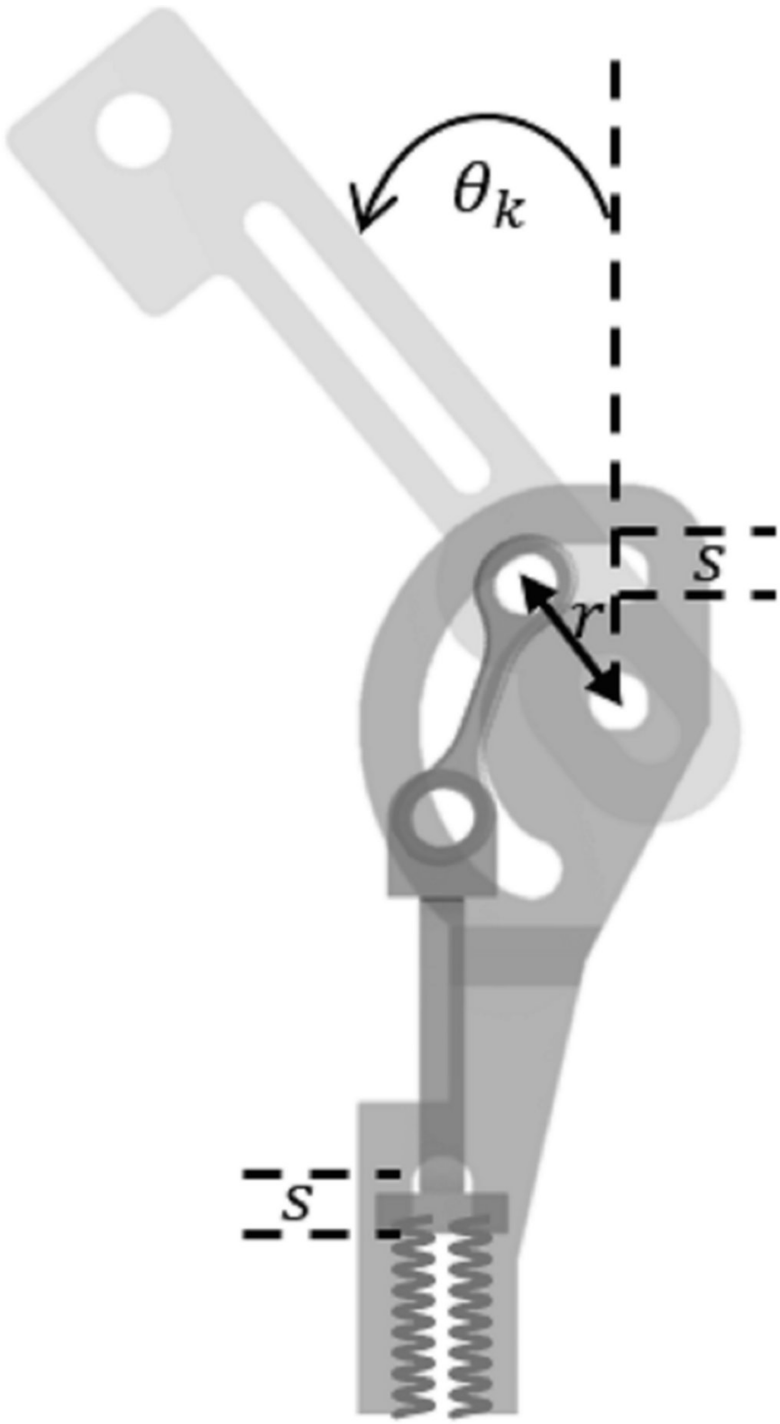

FIGURE 5: The schematic diagram of the KneExo and the corresponding cam slot

The configuration of the crank mechanism and the cam slot during the STS task is shown in Figure 5. Based on this figure, the deflection of the spring inside the shank can is determined according to the vertical displacement of the shank part along the cam slot as follows:

$$s = r(1 - \cos\theta_k)$$

Where s is the spring deflection during the stance phase of the STS task. Based on the generated force and moment arm vectors, the generated torque around the knee joint is determined as follows:

$$\vec{T} = \vec{r_m} \times \vec{F}$$

Where $\vec{r_m}$ and $\vec{F}$ are the moment arm and force vectors. Since the angle between the force vector and the moment arm is q_k, the generated torque is determined as follows:

$$T = Fr\cos\theta_k$$

As indicated in Figure *5*, the spring deflection depends only on the knee joint angle. A force-deflection graph, depicted in Figure *6*, is generated using the biological torque profile and torque and deflection equations to determine the elastic element's necessary stiffness for the KneExo in the full assistance condition.

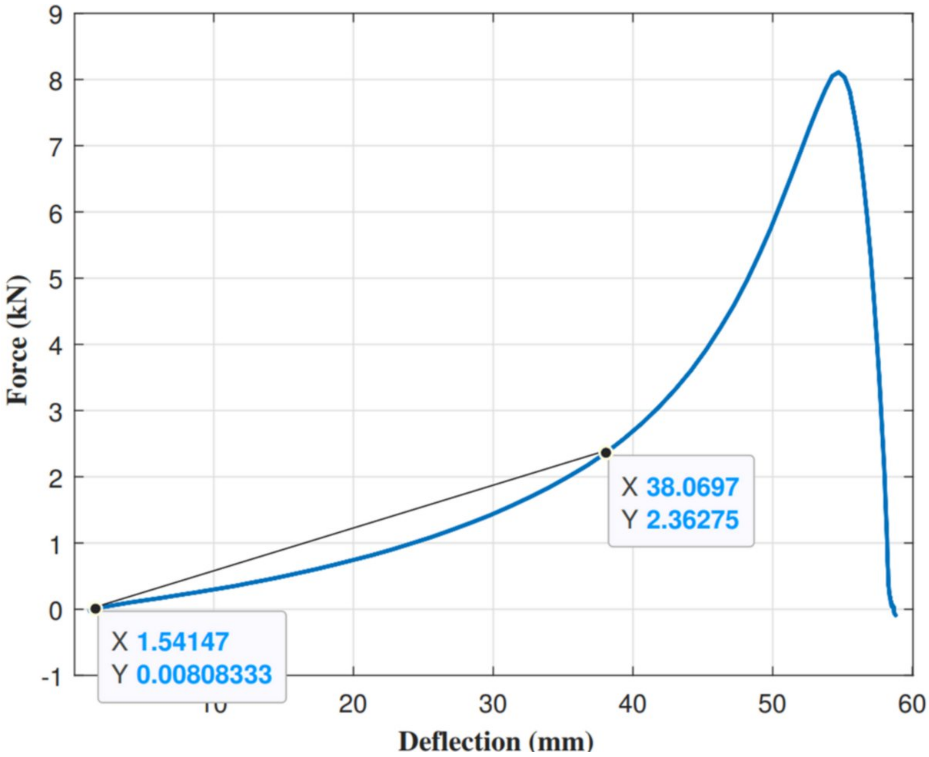

FIGURE 6: Force-deflection graph for full support mode

Here, the illustrated approach determines the spring stiffness for full support in the knee exoskeleton utilizing linear interpolation. To prevent excessively rigid springs and ensure the user's safety, the possibility of calculating the slope of linear interpolation between 30 mm and the maximum force point of Figure *6* at 56 mm is disregarded. Since the goal is to provide only 25% assistance due to reduced muscle strength in activities like standing from a chair, targeting an elastic constant of 16 N/mm would be sufficient to compensate for this loss. To achieve this, two parallel compression springs, each with 8 N/mm stiffness and a 58 mm stroke, are chosen, meeting the design parameters while ensuring functionality within specified limits: a maximum outer diameter of 12 mm and an initial length of 140 mm. This selected stiffness fulfills the desired assistance level and functionality within the exoskeleton's constraints, as depicted in Figure *7*, the simulation result of assistive torque with the determined springs.

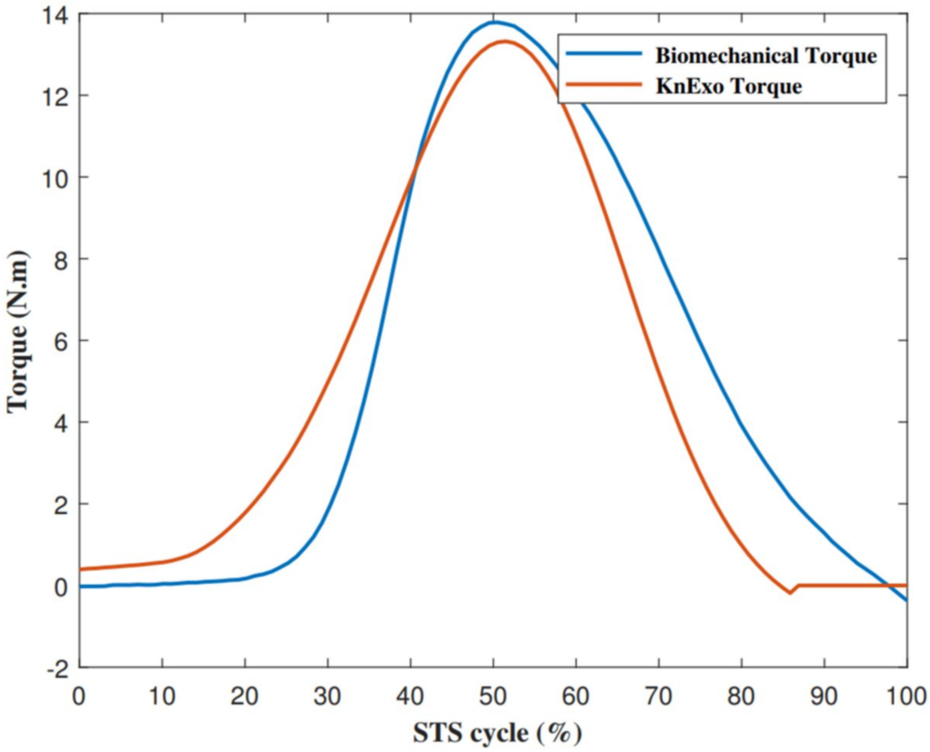

FIGURE 7: Performance simulation of the knee exoskeleton for 25% assistance

According to the simulation results, the proposed KneExo concept can provide 25% of the knee joint torque during the STS task with a 95.7% correlation and 1.71 N m RMS error.

Prototyping

The user's metabolic effort can be affected by the exoskeleton's mass. The selected material for manufacturing the KneExo should also have enough strength against the applied loads during the experiments. Hence, the material of the KneExo should be both lightweight and strong enough to perform the specified tasks. Al 7075 is a heat-treated alloy containing zinc, magnesium, and copper. This alloy's density and Young's module are 2.81 gr/cm^3 and 71.7 GPa [35,36], respectively, which is comparable to that of many steels while still being lightweight [37]. Therefore, using this material makes lightweight prototype manufacturing possible and provides a strong structure for conducting the experiments. Consequently, to realize the KneExo, the thigh and shank links, crank mechanism, and brace holders are manufactured from Al 7075. Rotational pins, linked via ball bearings (6700 ZZ), facilitate movement in the thigh and shank, as depicted in Figure *8* (left). Using the braces manufactured from formed plastics and the 3D-printed attachment parts (made from ABS), the KneExo is connected to the user's lower limbs. In Figure *8* (middle and right), the subject wears the KneExo prototype, attached to the lower limbs with braces and straps, and it is aligned with the user's knee joint.

FIGURE 8: Left: The rotational pins of the knee exoskeleton, middle: KneExo worn by the healthy subject—side view, Right: KneExo worn by the healthy subject—front view

The total mass of the exoskeleton is 2.25 kg for each leg, and the dimensions are $20 \times 24 \times 60cm$, being thickness, width, and height, respectively.

Results

The experiment of KneExo has been approved by the Clinical Research Ethics Committee of Istanbul Medipol University under document number E-10840098-772.02-6696. One of the authors of this study participated in the functional evaluations and confirmed the participation by signing the voluntary consent form.

Functional evaluation

A well-designed experimental setup is crucial for comprehensively evaluating the performance of the KneExo during the STS task. A standard office chair equipped with four load cells (KYOWA- LMB-A-2KN) placed on its armrests is used during the experiments. Contact points of the load cells and the hands are isolated by using 3D-printed parts to concentrate and measure all the applied forces from the hands on the armrests of the chair. Each load cell is statically calibrated before conducting the experiments, and the measured values are verified using known weights. Two load cells are used on each right and left armrest of the chair. Each load cell on the right and left armrests is connected to a 24-bit analog-to-digital converter (HX711, Avia Semiconductors, Xiamen, China). A microcontroller board (Arduino Mega 2560, Arduino LLC, USA) receives signals from the left and right load cells, with data acquisition occurring at 15 Hz. The kinematic data during experimental tests are collected using 7 IMU sensors (XSEN, MVN, The Netherlands) at a frequency of 100 Hz. The predefined model in the XSENS software is scaled based on the participant's lower-limb dimensions, and the IMU sensors are calibrated in advance. Additionally, to evaluate the selected muscles' activation during the experiments, a total of 8 sEMG Tringo sensors (DELSYS, USA) are employed to measure the muscle activation of the right and left quadriceps (QC), hamstrings (HS), tibialis anterior (TA), and gastrocnemius (GC) muscles synchronously with the kinematic data at a frequency of 2148 Hz. The selection of the QC, HS, TA, and GC muscles for evaluating the KneExo during the STS cycle is based on their critical roles in knee joint function and stability. The QC muscle is essential for knee extension and stability, while the HS muscle controls knee flexion and stability [38]. The TA muscle affects ankle dorsiflexion and foot positioning, and the GC muscle contributes to ankle propulsion [38].

The sEMG electrodes are placed based on the SENIAM recommendations [39]. The placement of the IMU and sEMG sensors on the subject is depicted in Figure *9*.

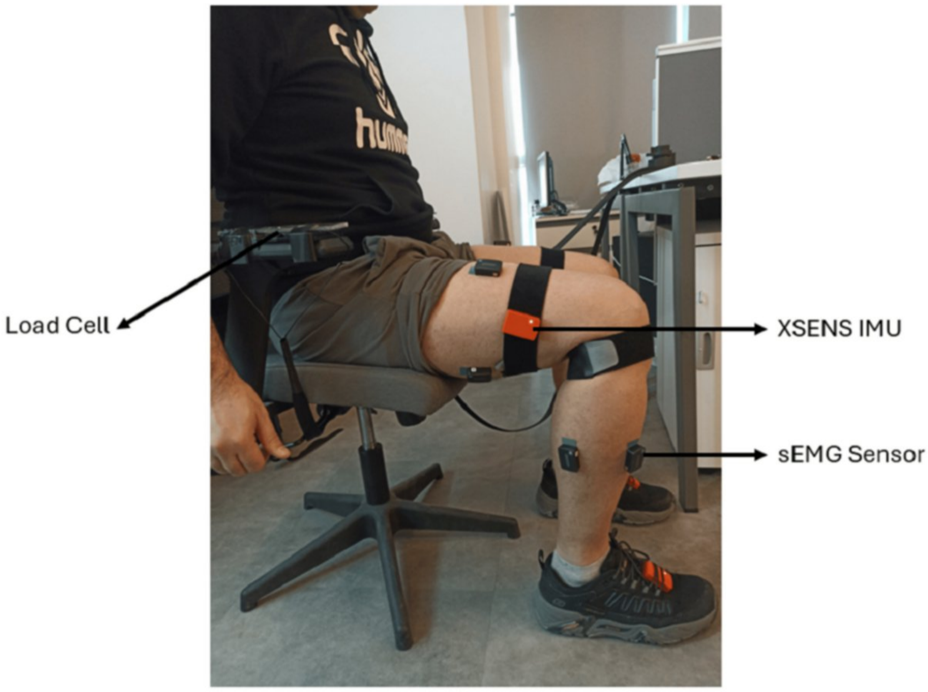

FIGURE 9: The placement of the load cells on the instrumented chair and the placement of the XSENS IMU and the sEMG sensors on the subject

A healthy individual, 175 cm in height and 80 kg in weight, participated in assessing the functionality of the KneExo. The STS cycle is performed in different scenarios. Unloaded and loaded scenarios with a 20 kg load, uniformly distributed within a backpack, are performed to collect the force, kinematic, and EMG data to evaluate the functionality of the KneExo. The loaded scenario is adopted to resemble the case of 25% assistance to older adults wearing the KneExo. To have a baseline for the measured data, the participant is asked to do the unloaded and loaded experiments without wearing the KneExo.

Additionally, the subject repeats the experiments with and without exoskeleton assistance conditions, encompassing both loaded and unloaded STS cycles. This evaluation allows for a comprehensive comparison of force data between various conditions to understand the efficacy of the KneExo under different loads and assistance modes. Before starting the experiments, the maximum voluntary contraction (MVC) of each muscle is recorded through full knee joint flexion and squat movements while the participant wears the KneExo in the unloaded case. Based on the type of experiments, the performing time for each cycle varies between 4.3 s and 6.5 s.

To ensure consistency in the collected data and reduce the impact of any individual outliers or disturbances, the participant was asked to perform each task five times, allowing us to obtain a reliable average for preliminary insights. Graphical representations illustrate load-bearing modes (with/without backpack load) assisted by the exoskeleton (AE) and without exoskeleton assistance (NoAE), facilitating a comprehensive analysis of the results. A video of the functional evaluation of the KneExo during the AE scenario for the unloaded and loaded cases is shown in Video *1*.

VIDEO 1: The functional evaluation of the KneExo during the AE scenario for the unloaded and loaded cases

View video here: https://www.youtube.com/watch?v=Bdzr3cljL64

Since the sit-to-stand-to-sit (STSTS) cycle captures the complete range of motion of the knee joint, from flexion to extension and back to flexion hence, it allows for a thorough assessment of the exoskeleton's kinematic ability. Therefore, the STSTS results are reported only for the knee joint angle. Furthermore, the STS phase is the most physically demanding part of the movement, where muscle activation and exoskeleton assistance are critical for overcoming inertia and lifting the body. Focusing on this phase allows for a clearer assessment of the KneExo's effectiveness in reducing the activities of muscles and assistive force by the hands during a key functional task. The average knee angle of five STSTS cycles for the NoAE scenario is depicted in Figure *10*.

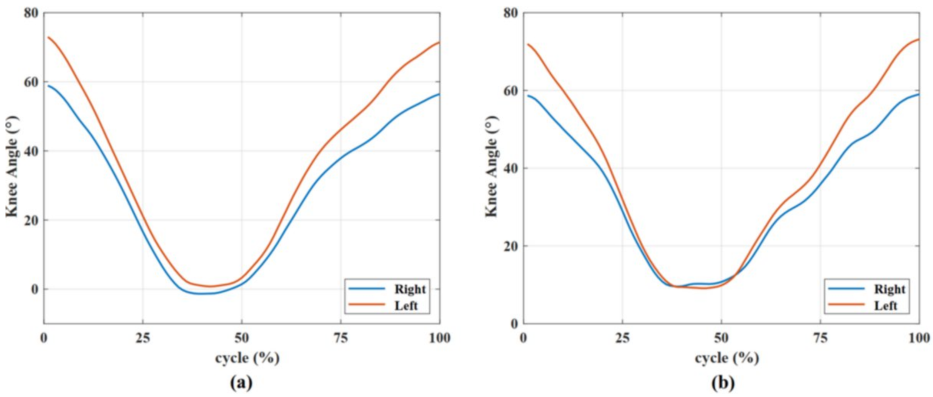

FIGURE 10: The average knee angle of five sit-to-stand-sit cycles for the NoAE scenario in unloaded (a) and loaded (b) cases

Here, the maximum flexion angles in the right knee joint are 58.9° and 58.7° for the unloaded and loaded cases, respectively. Also, the maximum flexion angles in the right knee joint are 73° and 72° for the unloaded and loaded cases, respectively. Additionally, the average knee angle of five STSTS cycles for the AE scenario is depicted in Figure *11*.

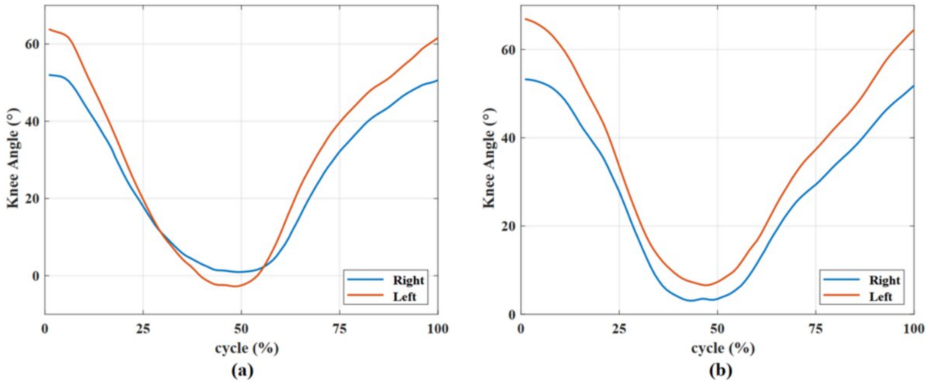

FIGURE 11: The average knee angle of five sit-to-stand-sit cycles for the AE scenario in unloaded (a) and loaded (b) cases

The initial results of the KneExo show that the maximum flexion angles in the right knee joint are 52° and 53.25° for the unloaded and loaded cases, respectively. Also, the maximum flexion angles in the right knee joint are 68.3° and 66.9° for the unloaded and loaded cases, respectively. The duration of the STSTS cycles for the unloaded and loaded cases of the AE scenario are 6 s and 6.5 s, respectively. Also, the duration of the STSTS cycles for the unloaded and loaded cases of the NoAE scenario are 5.5 s and 5.8 s, respectively.

Since the assistance of the KneExo appears during the STS phase, only the measured forces exerted by the left and right hands throughout stand-to-sit-stand cycles are reported in this study. In Figure *12*, the average forces from the left and right hands during the STS cycle of the unloaded case for the baseline, AE, and NoAE scenarios are shown.

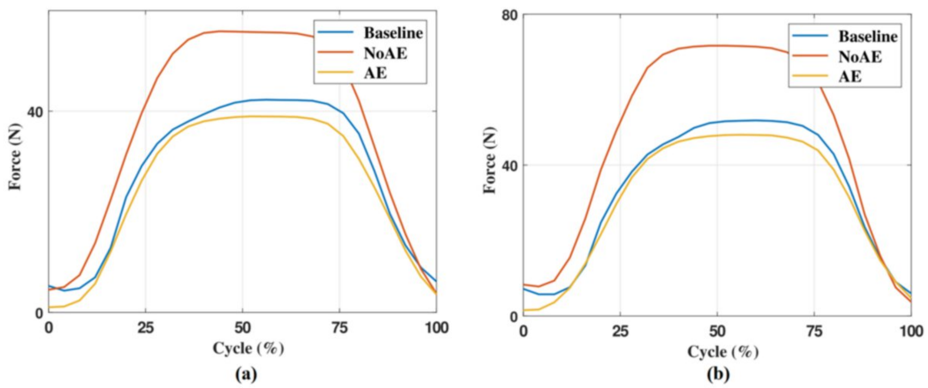

FIGURE 12: The average forces from the left (a) and right (b) hands of the unloaded case for the baseline, AE, and NoAE scenarios

Here, the maximum average values for the left hand in the unloaded case are 42.3 N, 38.9 N, and 55.8 N for the baseline, AE, and NoAE scenarios, respectively. Additionally, these values for the right hand are 51.8 N, 48.1 N, and 71.6 N for the baseline, AE, and NoAE scenarios, respectively. In Figure *13*, the average forces from the left and right hands during the STS cycle of the loaded case for the baseline, AE, and NoAE scenarios are shown.

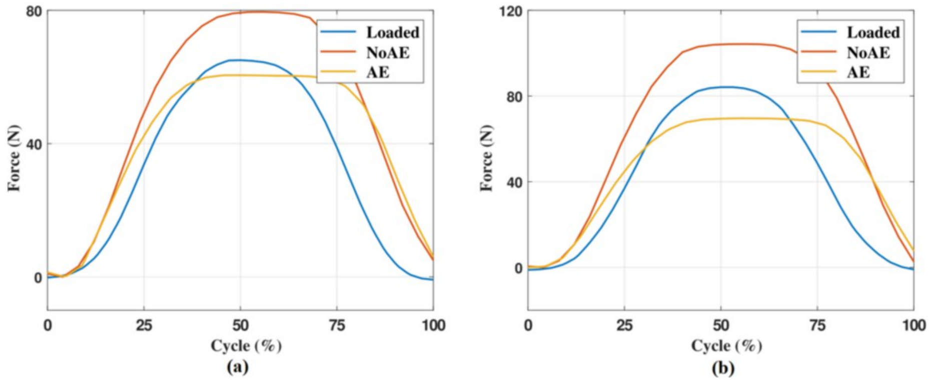

FIGURE 13: The average forces from the left (a) and right (b) hands of the loaded case for the baseline, AE, and NoAE scenarios

Here, the maximum average values for the left hand in the loaded case are 65 N, 60.4 N, and 79.5 N for the baseline, AE, and NoAE scenarios, respectively. These values for the right hand are 84.1 N, 69.6 N, and 104.2 N for the baseline, AE, and NoAE scenarios, respectively. The average of total forces from the right and left hands for the loaded and unloaded cases of different scenarios are depicted in Figure *14*.

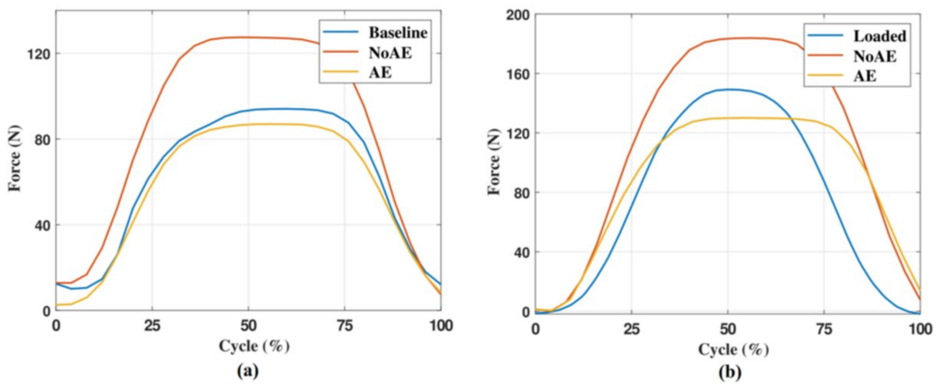

FIGURE 14: The average total forces of the unloaded (a) and loaded (b) cases for the baseline, AE, and NoAE scenarios

Here, the maximums of the average value for the total forces of the unloaded case are 94.1 N, 86.9 N, and 127.3 N for the baseline, AE, and NoAE scenarios, respectively. Additionally, the maximums of the average value for the total forces in the loaded case are 149.1 N, 130.1 N, and 183.7 N for the baseline, AE, and NoAE scenarios, respectively.

The smoothed rectified envelope of the raw EMG data of the eight muscles is obtained by considering a cut-off frequency in the range of 20-450, rectifying and low-pass filtering at 6 Hz. All muscle activations are normalized based on the recorded MVC values. The average muscle activation results during five STS cycles for the unloaded and loaded cases are depicted in Figure *15*.

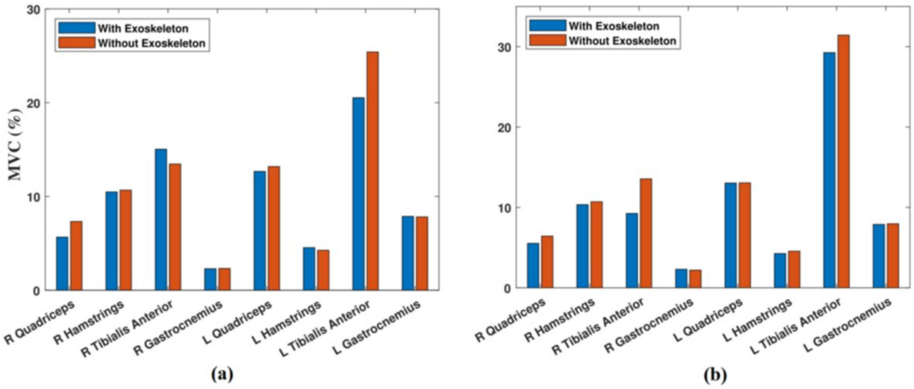

FIGURE 15: The average activation of the muscles for the unloaded (a) and loaded (b) cases.

Here, the blue and red bar graphics represent the scenarios with and without assistance from the KneExo, respectively. In the unloaded case for the selected muscles, the maximum muscle activation during the STS task is 31.43% for the left TA muscle for the loaded case in the NoAE scenario. Also, the minimum muscle activation during the STS task is 2.2% for the right GC muscle for the loaded case in the NoAE scenario. In the unloaded cases, the muscle activation of the QC and HS muscles of the right leg and muscle activation of the QC and TA muscles of the left leg in the AE scenario are lower than these values in the NoAE scenario. In this case, both scenarios show no obvious difference in muscle activation of the right and left GC muscles. In the unloaded case, the muscle activation of the QC, TA, and GC muscles in the left leg is more than that of the right leg for both scenarios. In the loaded case, the muscle activation of the QC, HS, and TA muscles of the right leg and muscle activation of the HS and TA muscles of the left leg in the AE scenario are lower than these values in the NoAE scenario. In the unloaded and loaded cases, the muscle activation of the QC, TA, and GC muscles in the left leg is more than that of the right leg for both scenarios. Both scenarios show no obvious difference in the loaded case muscle activation of the right and left GC and left QC muscles. The detailed results of the measured activation of each muscle for different loading cases and scenarios are listed in Table *1*.

Loading/scenario	Unloaded (% of MVC)		Loaded (% of MVC)	
Right QC	5.6	7.33	5.53	6.43
Right HS	10.48	10.67	10.35	10.71
Right TA	15.03	13.46	9.25	13.56
Right GC	2.3	2.32	2.3	2.2
Left QC	12.67	13.19	13.03	13.06
Left HS	4.55	4.26	4.26	4.56
Left TA	20.52	25.4	29.26	31.43
Left GC	7.87	7.82	7.89	7.96

TABLE 1: Activation of each muscle during AE and NoAE scenarios

Misalignment evaluation

Two markers are placed on both the subject and the knee joint of the exoskeleton to measure the alignment discrepancies between them. These markers are positioned in a manner ensuring their axes align when both the subject and exoskeleton are in a standing position. The 3D positional data of these markers are recorded using five motion capture cameras (NaturalPoint, Inc. DBA OptiTrack, USA), operating at a sample rate of 50 measurements per second. Misalignment between the subject's knee and the exoskeleton's knee joint is quantified by examining the difference in the longitudinal data of these two markers.

These tests are conducted five times, with each STS cycle lasting 5 s. In this study, the average of these cycles is being reported. To facilitate a comparison between the misalignment results of the KneExo and those with a revolute joint, the knee exoskeleton is considered a 3DOF linkage system, with the foot assumed to be fixed on the ground during the STS cycle. Consequently, the longitudinal position of the knee joint is determined as follows:

$$P_x = l_f \sin q_a + l_k \sin (q_a + q_k)$$

Where l_f and l_k are the foot and shank link lengths, and q_a and q_k are the ankle and knee angles during the STS cycle. The results of these two designs are shown in Figure *16*.

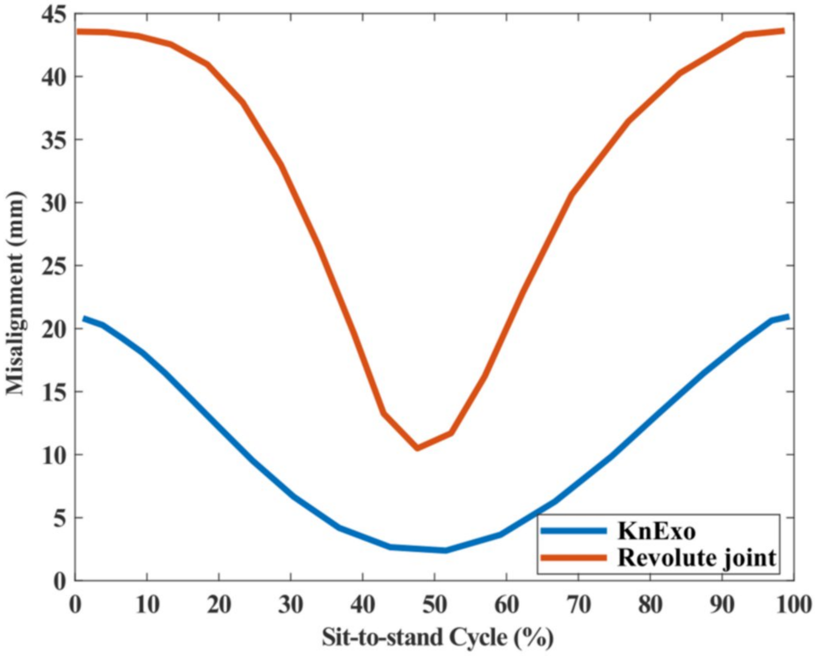

FIGURE 16: The comparison of the misalignment in the bio-shaped and revolute-joint knee exoskeletons

Here, in the standing position, the misalignment is considered the minimum value. The revolute joint's misalignment starts at 43 mm in the sitting position, while the misalignment of the KneExo starts from 21 mm. Based on this comparison, it can be observed that the misalignment reduction is 51%. According to the experiment and simulation results for the misalignment assessment of the KneExo and those with the revolute joint, the misalignment during the standing position is 10 mm for the revolute joint concept and 2 mm in the KneExo design.

Discussion

In this study, the design, development, and functional evaluation of the initial prototype of the KneExo are presented. In comparison to the Quasi-Passive Knee Exoskeleton [14], the proposed KneExo prototype is 40% lighter. Although the total mass of the KneExo is 5.6% of the participant's weight, using the 3D-printed composite material would reduce the weight of the KneExo for the target population. According to the preliminary results obtained during the functional evaluations of the KneExo, the practical utility of this exoskeleton is evident in the considerable reduction of the required total force from the hands during the STS cycle. In other words, the KneExo can considerably lessen the effort required for a subject to transition from a seated position to a standing one. According to the initial functional evaluation results using the KneExo, 30.2% and 33% less assistance is needed from the left and right hands for the unloaded case, and 23.9% and 33.3% less assistance is needed from the left and right for the loaded case during the STS. Additionally, using the KneExo actively during the experiments, the total assistance from the hand forces in the loaded and unloaded cases can be reduced by 31.76% and 29.24%, respectively. The initial results of the KneExo indicate that the AE mode reduces peak forces in both hands during the STS cycle. Moreover, the duration of force application appears slightly extended, as seen in the longer plateau of the load curve for the AE scenario compared to NoAE. This extended plateau suggests that the KneExo, when active, distributes the required effort over a longer period, which could potentially enhance comfort and reduce fatigue for the user. The collected data from load cells during the functional evaluations reveal that the subject exerts 2.7% more force with the right hand in the unloaded case and 9.4% more force during the loaded case. Since the participant's dominant hand is the right hand, applying extra force with the right hand during STS might result from this fact. Additionally, the reason for the less required assistance in the right hand to perform the STS cycle might be the better functionality of the KneExo on the right side. The total assistance provided by the KneExo in the loaded case is less than that provided in the unloaded case since the elastic elements are designed for an 80 kg subject. Although the design of the elastic elements aims to assist the participant by compensating for muscle weakness, when additional mass is introduced, the level of assistance provided by the KneExo decreases relative to the body mass. Moreover, due to the required energy for sitting and overcoming the spring forces, according to the results, the knee joint's RoM in the AE scenario is less than that in the NoAE scenario. Adding extra stiffness to the KneExo would assist the participant more during the STS cycle, but the task during the sitting phase would be more challenging. The KneExo can, therefore, be equipped with an engage/disengage mechanism to deactivate the spring force while the participant's sitting area is in contact with the chair.

According to the initial EMG results during the STS task, the HS and TA muscles are most activated in the right leg, and the QC and TA muscles are most activated in the left leg. Since the assistance from the right hand is greater during the STS cycle, more activation of TA and QC muscles of the left leg might result. As the hands finish their contact with the armrest of the chair, the TA muscles are activated, and the transition phase of the STS is started. As a result, the most reduction is seen in these muscles when using the KneExo. Therefore, for the unloaded case, a reduction of 19.2% muscle activation in the left TA muscle and a reduction of 31.2 muscle activation for the loaded case happens in the right TA muscle by 31.2% in the AE scenario. Although these initial observations suggest that asymmetrical assistance may influence muscle activation patterns, further studies with a larger participant sample are necessary to confirm and statistically validate these effects. These preliminary findings provide insights that will guide future, more comprehensive evaluations of the KneExo. According to the kinematics results during the tasks, it is observed that the left knee joint performs 22.7% and 25.7% more flexion than the right knee joint in the unloaded and loaded cases, respectively. Several factors may influence this difference in knee joint flexion between the two legs. One possible reason could be the different functional performances of the KneExo mechanisms on the right and left sides.

Additionally, using the hands on the armrests and the dominant hand effect during the STS task may alter the distribution of forces and affect the movement pattern. Variations in the dominant leg and hand, as well as individual STS posture and technique, might also contribute to these differences in knee joint flexion. Additionally, as observed during these evaluations, more flexion in the left knee joint might result in more muscle activation of the left QC and TA muscles than those in the right leg. Therefore, in future studies, it might be necessary to individualize the designs based on the dominant side rather than symmetrical designs for the users.

The 51% reduction in the misalignment results of the bio-joint shaped knee mechanism, compared with the conventional revolute joint, demonstrate that accounting for both rotational and translational movements-as in human knee biomechanics-enables a more accurate emulation of knee function in the exoskeleton. Observed misalignments may arise from prototype limitations or individual biomechanical variations, such as ankle and knee angles during STS, given that the CAM slot is designed based on specific anatomical data. This approach aligns with findings in the literature [25], where implementing a bio-inspired joint in the exoskeleton reduced pressure by 30%, resulting in less misalignment and enhanced user comfort.

One of the mechanical constraints of the proposed KneExo is its ability to provide a 90° flexion in the knee joint during STS cycles. By modifying the design, the KneExo would be able to perform full flexion during the STS task and provide more assistance to the subject. During the STS task, although the KneExo design provides zero torque around the knee joint during sitting by adjusting the moment arm, the spring should be locked in this phase to avoid unwanted release of the spring energy during sitting. In this study, only STS activity is investigated, whereby adding a mechanism in the foot to engage and disengage the spring mechanism can make this device to be employed during walking, as well. Additionally, this study presents the initial prototype of the KneExo for functional evaluation purposes, which is mainly made from AL. Significant mass and volume reduction would be achieved by using 3D-printed parts, such as plastic reinforced by carbon fiber or tough Polylactic Acid.

Conclusions

Improving mobility in elderly populations through technologies like the KneExo exoskeleton can significantly reduce healthcare burdens by enhancing independence and preventing mobility-related health issues. This study presents the design, development, and functional evaluation of a bio-joint shaped knee exoskeleton capable of storing energy while sitting and releasing it to assist while standing. Based on the rotational and translational movement of the knee joint during the ADL, the cam slot is designed to compensate for the misalignment of the knee joint. The prototype of the KneExo is manufactured from Al, and its mass is 2.25 kg. According to the results of the functional evaluation, it is observed that using the KneExo results in 31.8% and 29% reduction in the total hand forces during the STS cycle for the unloaded and loaded cases, respectively. The EMG results reveal that while the participant uses the KneExo during the STS tasks, there is a 19.2% reduction in the muscle activation of the left TA muscle for the unloaded case and a 31.2% reduction in the muscle activation of the right TA for the loaded case. The misalignment between the knee joint of the KneExo and the participant is also evaluated. Compared to a revolute joint, the proposed KneExo, using the cam slot that mimics the human biomechanics, showcases a considerable decrease of 51% in misalignment with the user's knee joint. In the future, implementing a dis/engaging mechanism to enable this knee exoskeleton for walking assistance would benefit elderly people and industrial workers during their daily activities. We would also like to evaluate this exoskeleton with more subjects to show the device's efficacy more generically. After these evaluations and improvements on the design of the KneExo, it would be necessary to evaluate the device's efficacy with its end-users to put it into service for elderly people to improve the quality of their lives.

Additional Information

Author Contributions

All authors have reviewed the final version to be published and agreed to be accountable for all aspects of the work.

Concept and design: Omid Arfaie, Ramazan Unal

Acquisition, analysis, or interpretation of data: Omid Arfaie, Ramazan Unal

Drafting of the manuscript: Omid Arfaie, Ramazan Unal

Critical review of the manuscript for important intellectual content: Omid Arfaie, Ramazan Unal

Supervision: Ramazan Unal

Disclosures

Human subjects: Consent was obtained or waived by all participants in this study. Clinical Research Ethics Committee of Istanbul Medipol University issued approval E-10840098-772.02-6696. The experiment of KneExo has been approved by the Clinical Research Ethics Committee of Istanbul Medipol University under document number E-10840098-772.02-6696. One of the authors of this study participated in the functional evaluations and confirmed the participation by signing the voluntary consent form. **Animal subjects:** All authors have confirmed that this study did not involve animal subjects or tissue. **Conflicts of interest:** In compliance with the ICMJE uniform disclosure form, all authors declare the following: **Payment/services info:** All authors have declared that no financial support was received from any organization for the submitted work. **Financial relationships:** All authors have declared that they have no financial relationships at present or within the previous three years with any organizations that might have an interest in the submitted work. **Other relationships:** All authors have declared that there are no other relationships or activities that could appear to have influenced the submitted work.

References

1. World Health Organization, Ageing and Health. (2022). Accessed: March 15, 2024: https://www.who.int/news-room/fact-sheets/detail/ageing-and-health.
2. Nakano MM, Otonari TS, Takara KS, Carmo CM, Tanaka C: Physical performance, balance, mobility, and muscle strength decline at different rates in elderly people. Journal of Physical Therapy Science. 2014, 26:583-86. 10.1589/jpts.26.583
3. Muehlbauer T, Gollhofer A, Granacher U: Associations between measures of balance and lower-extremity muscle strength/power in healthy individuals across the lifespan: a systematic review and meta-analysis. Sports Medicine. 2015, 45:1671-92. 10.1007/s40279-015-0390-z
4. Batista FS, Gomes GADO,Neri AL, Guariento ME, Cintra FA, Sousa MDLRD, D'Elboux MJ: Relationship between lower-limb muscle strength and frailty among elderly people. Sao Paulo Medical Journal. 2012, 130:102-8. 10.1590/s1516-31802012000200006
5. Hurley BF: Age, gender, and muscular strength. Journals of Gerontology Series A: Biomedical Sciences and Medical Sciences. 1995, 50A:41-44. 10.1093/gerona/50a.special_issue.41
6. Cuesta-Vargas AI, González-Sánchez M: Differences in muscle activation patterns during sit to stand task among subjects with and without intellectual disability. BioMed Research International. 2013, 2013:1-7. 10.1155/2013/173148
7. Rosales-Díaz I, López-Gutiérrez JR, Suárez AEZ, Salazar SR, Osorio-Cordero A, Aguilar-Sierra H, Lozano R: Comparison of control techniques in a weight lifting exoskeleton. Journal of Bionic Engineering. 2019, 16:663-73. 10.1007/s42235-019-0053-0
8. Luger T, Seibt R, Cobb TJ, Rieger MA, Steinhilber B: Influence of a passive lower-limb exoskeleton during simulated industrial work tasks on physical load, upper body posture, postural control and discomfort. Applied Ergonomics. 2019, 80:152-60. 10.1016/j.apergo.2019.05.018
9. Zhou L, Chen W, Chen W, Bai S, Zhang J, Wang J: Design of a passive lower limb exoskeleton for walking assistance with gravity compensation. Mechanism and Machine Theory. 2020, 150:103840. 10.1016/j.mechmachtheory.2020.103840
10. Kong K, Jeon D: Design and control of an exoskeleton for the elderly and patients. IEEE/ASME Transactions on Mechatronics. 2006, 11:428-32. 10.1109/tmech.2006.878550
11. Beyl P, Knaepen K, Duerinck S, Van Damme M, Vanderborght B, Meeusen R, Lefeber D: Safe and compliant

guidance by a powered knee exoskeleton for robot-assisted rehabilitation of gait. Advanced Robotics. 2011, 25:513-35. 10.1163/016918611x558225

12. Kong K, Bae J, Tomizuka M: A compact rotary series elastic actuator for human assistive systems. IEEE/ASME Transactions on Mechatronics. 2012, 17:288-97. 10.1109/tmech.2010.2100046
13. Shepherd MK, Rouse EJ: Design and validation of a torque-controllable knee exoskeleton for sit-to-stand assistance. IEEE/ASME Transactions on Mechatronics. 2017, 22:1695-704. 10.1109/tmech.2017.2704521
14. Shamaei K, Cenciarini M, Adams AA, Gregorczyk KN, Schiffman JM, Dollar AM: Design and evaluation of a quasi-passive knee exoskeleton for investigation of motor adaptation in lower extremity joints. IEEE Transactions on Biomedical Engineering. 2014, 61:1809-21. 10.1109/tbme.2014.2307698
15. Ortiz J, Poliero T, Cairoli G, Graf E, Caldwell DG: Energy efficiency analysis and design optimization of an actuation system in a soft modular lower limb exoskeleton. IEEE Robotics and Automation Letters. 2018, 3:484-91. 10.1109/lra.2017.2768119
16. Debeurre M, Thalman CM, Hertzell T, Lee H: Soft robotic AFO for active stroke rehabilitation. 3rd IEEE International Conference on Soft Robotics. 2020, 10.13140/RG.2.2.35141.19688
17. Esquenazi A, Talaty M, Packel A, Saulino M: The ReWalk powered exoskeleton to restore ambulatory function to individuals with thoracic-level motor-complete spinal cord injury. American Journal of Physical Medicine & Rehabilitation. 2012, 91:911-21. 10.1097/phm.0b013e318269d9a3
18. Chen B, Zhong CH, Zhao X, et al.: A wearable exoskeleton suit for motion assistance to paralysed patients. Journal of Orthopaedic Translation. 2017, 11:7-18. 10.1016/j.jot.2017.02.007
19. Sawicki GS, Ferris DP: A pneumatically powered knee-ankle-foot orthosis (KAFO) with myoelectric activation and inhibition. Journal of NeuroEngineering and Rehabilitation. 2009, 6:23. 10.1186/1743-0003-6-23
20. Granados DFP, Kadone H, Suzuki K: Unpowered lower-body exoskeleton with torso lifting mechanism for supporting sit-to-stand transitions. 2018 IEEE/RSJ International Conference on Intelligent Robots and Systems (IROS). 2018, 2755-61. 10.1109/IROS.2018.8594199
21. Iwaki H, Pinskerova V, Freeman MAR: Tibiofemoral movement 1: the shapes and relative movements of the femur and tibia in the unloaded cadaver knee. Journal of Bone and Joint Surgery. 2000, 82:1189-95. 10.1302/0301-620x.82b8.10717
22. Li Y, Chang SH, Francisco G, Su H : Interaction force modeling for joint misalignment minimization toward bio-inspired knee exoskeleton design. Proceedings of the 2018 Design of Medical Devices Conference DMD2018. 2018, V001T10A011. 10.1115/DMD2018-6921
23. Zanotto D, Akiyama Y, Stegall P, Agrawal SK: Knee joint misalignment in exoskeletons for the lower extremities: effects on user's gait. IEEE Transactions on Robotics. 2015, 31:978-87. 10.1109/tro.2015.2450414
24. Sarkisian SV, Ishmael MK, Lenzi T: Self-aligning mechanism improves comfort and performance with a powered knee exoskeleton. IEEE Transactions on Neural Systems and Rehabilitation Engineering. 2021, 29:629-40. 10.1109/tnsre.2021.3064463
25. Kim T, Jeong M, Kong K: Bioinspired knee joint of a lower-limb exoskeleton for misalignment reduction. IEEE/ASME Transactions on Mechatronics. 2022, 27:1223-32. 10.1109/tmech.2021.3099815
26. Hyun DJ, Park H, Ha T, Park S, Jung K: Biomechanical design of an agile, electricity-powered lower-limb exoskeleton for weight-bearing assistance. Robotics and Autonomous Systems. 2017, 95:181-95. 10.1016/j.robot.2017.06.010
27. Li G, Liang X, Lu H, Su T, Hou ZG: Development and validation of a self-aligning knee exoskeleton with hip rotation capability. IEEE Transactions on Neural Systems and Rehabilitation Engineering. 2024, 32:472-81. 10.1109/tnsre.2024.3354806
28. Wang D, Lee KM, Guo J, Yang CJ: Adaptive knee joint exoskeleton based on biological geometries. IEEE/ASME Transactions on Mechatronics. 2014, 19:1268-78. 10.1109/tmech.2013.2278207
29. Kapci MF, Unal R: Design of bio-joint shaped knee exoskeleton assisting for walking and sit-to-stance. International Symposium on Wearable Robotics. 2018, 495-99. 10.1007/978-3-030-01887-0_96
30. Gilleard W, Crosbie J, Smith R: Rising to stand from a chair: symmetry, and frontal and transverse plane kinematics and kinetics. Gait & Posture. 2008, 27:8-15. 10.1016/j.gaitpost.2006.11.002
31. Pinheiro C, Lopes JM, Moreira L, Sanz-Merodio D, Figueiredo J, Santos CP, Garcia E: Kinematic and kinetic study of sit-to-stand and stand-to-sit movements towards a human-like skeletal model. 2019 IEEE 6th Portuguese Meeting on Bioengineering (ENBENG). 2019, 10.1109/ENBENG.2019.8692569
32. Lee KM, Guo J: Kinematic and dynamic analysis of an anatomically based knee joint. Journal of Biomechanics. 2010, 43:1231-36. 10.1016/j.jbiomech.2010.02.001
33. Hamai S, Moro-oka TA, Dunbar NJ, Miura H, Iwamoto Y, Banks SA: In vivo healthy knee kinematics during dynamic full flexion. BioMed Research International. 2013, 2013:717546. 10.1155/2013/717546
34. Kainz H, Graham D, Edwards J, et al.: Reliability of four models for clinical gait analysis. Gait & Posture. 2017, 54:325-31. 10.1016/j.gaitpost.2017.04.001
35. Sistiaga MLM, Mertens R, Vrancken B, Wang X, Van Hooreweder B, Kruth JP, Van Humbeeck J: Changing the alloy composition of Al7075 for better processability by selective laser melting. Journal of Materials Processing Technology. 2016, 238:437-45. 10.1016/j.jmatprotec.2016.08.003
36. Aghajani S, Pouyafar V, Meshkabadi R, Volinsky AA, Bolouri A: Mechanical characterization of high volume fraction Al7075-Al2O3 composite fabricated by semisolid powder processing. The International Journal of Advanced Manufacturing Technology. 2023, 125:2569-80. 10.1007/s00170-023-10881-9
37. Kumar PV, Reddy GM, Rao KS: Microstructure, mechanical and corrosion behavior of high strength AA7075 aluminium alloy friction stir welds - Effect of post weld heat treatment. Defence Technology. 2015, 11:362-69. 10.1016/j.dt.2015.04.003
38. Özkaya N, Nordin M, Goldsheyder D, Leger D: Fundamentals of Biomechanics. Springer, New York; 2012. 10.1007/978-3-319-44738-4
39. Hermens HJ, Freriks B, Disselhorst-Klug C, Rau G: Development of recommendations for sEMG sensors and sensor placement procedures. Journal of Electromyography and Kinesiology. 2000, 10:361-74. 10.1016/s1050-6411(00)00027-4